THE JOURNAL OF BIOLOGICAL CHEMISTRY
Vol. 264, No. 31, Issue of November 5, pp. 18751-18760, 1989
Printed in U.S.A.

Site-specific Substitution of Glutamate for Aspartate at Position 59 of Rat Oncomodulin*

(Received for publication, May 4, 1989)

Raymond C. Hapak, Peter J. Lammers, William A. Palmisano, Edward R. Birnbaum, and Michael T. Henzl‡

From the Department of Chemistry, New Mexico State University, Las Cruces, New Mexico 88003

Replacement of the aspartate residue at position 59 of rat oncomodulin by glutamate by oligonucleotide-directed mutagenesis has afforded a protein which more closely resembles rat parvalbumin, at least judged by its interaction with the luminescent lanthanide ion Eu^{3+}. The single-peak $^7F_0 \rightarrow {}^5D_0$ spectrum observed at pH 5.0 with the fully bound wild-type protein is replaced by one which clearly shows two features at 5791 and 5796 Å, arising from Eu^{3+} ions bound at the CD and EF sites, respectively. Furthermore, the pH dependence of the spectrum is substantially altered; the pK_a observed for the CD domain, in which aspartate 59 resides, is shifted upward from pH 6.0 for the wild-type recombinant protein to pH 6.8 in the D59E mutant. Moreover, the maximum in the high-pH spectrum is shifted from 5781 to 5784 Å. All three changes are indicative of a CD binding domain having increased parvalbumin-like character. Interestingly, however, the D59E substitution has only a modest effect on the Ca^{2+}-and Mg^{2+}-binding properties of the CD domain. For the wild-type protein, $K_{Ca} = 7.8 \times 10^{-7}$ M and $K_{Mg} = 3 \times 10^{-3}$ M. These affinities are more than an order of magnitude weaker than those seen for various parvalbumins and substantiate previous claims for calcium specificity made for the oncomodulin CD domain. Replacement of aspartate 59 by glutamate resulted in minor increases in affinity of the CD domain for Ca^{2+} ($K_{Ca} = 5.5 \times 10^{-7}$ M) and Mg^{2+} ($K_{Mg} = 1 \times 10^{-3}$ M). These findings strongly suggest that residues in oncomodulin besides aspartate 59 are important determinants of the observed calcium specificity of the CD calcium-binding domain. The consequences of the substitution at residue 59 appear to be confined to the CD domain. For the EF site in wild-type recombinant oncomodulin, $K_{Ca} = 4.2 \times 10^{-8}$ M and $K_{Mg} = 1.6 \times 10^{-4}$ M. The corresponding values for the D59E site-specific variant are identical within experimental error ($K_{Ca} = 4.2 \times 10^{-8}$ M and $K_{Mg} = 1.8 \times 10^{-4}$ M).

The calcium ion-binding domains characteristic of intracellular calcium-binding proteins share a common structural motif, which consists of a 10-residue loop flanked by 10-residue stretches of α-helix (1, 2). Coordination of the bound Ca^{2+} ion is approximately octahedral with five of the six ligands donated by residues within the loop and the sixth ligand donated by a proximal residue in the COOH-terminal helix. This motif has been labeled the "EF hand" by Kretsinger (3), the spatial relationship of the flanking helices resembling that between the outstretched thumb and forefinger of the right hand. First observed in carp parvalbumin, EF hands have subsequently been observed in the crystal structures of bovine intestinal calcium-binding protein (4), skeletal troponin C (5, 6), and calmodulin (7).

Calcium ion-binding domains can be divided into two classes on the basis of their affinity for Mg^{2+} (1, 2, 8, 9). Those which display affinity for both Ca^{2+} and Mg^{2+} at physiological pH and ionic strength are said to be "Ca^{2+}/Mg^{2+}" sites, while those having negligible affinity for Mg^{2+} under physiological conditions are said to be "Ca^{2+} specific." Ca^{2+}-specific sites occur in proteins which trigger physiological phenomena. For example, two of the four domains in skeletal troponin C and all four of the sites in calmodulin fall into this category. Ca^{2+}/Mg^{2+} sites, on the other hand, are believed to play a more passive role, acting as Ca^{2+} buffers. Parvalbumin, a muscle-associated protein containing two Ca^{2+}/Mg^{2+}-binding domains, is believed to function in the relaxation of fast-twitch skeletal muscle. Despite extensive investigation, the ultimate origin of specificity in calcium ion-binding domains is not completely understood.

Oncomodulin, the parvalbumin-like calcium-binding protein first described and characterized by MacManus and Whitfield (10), represents a potentially useful system in which to examine this question. Named for its frequent association with neoplastic tissue (10–12) and its ability to stimulate cyclic nucleotide phosphodiesterase in a manner reminiscent of calmodulin (13, 14), oncomodulin is normally expressed only in the cytotrophoblast of fetal placental tissue (15–17). The protein is unusual in that it pairs a single Ca^{2+}-specific site (the CD site)[1] with a single Ca^{2+}/Mg^{2+} site (the EF site) (18–20). We have embarked upon a program of site-directed mutagenesis aimed at identifying residues in the protein that are critical to the calcium specificity of the CD domain. To this end, we have cloned and expressed the oncomodulin coding sequence in *Escherichia coli* and have initiated oligo-

* This work was supported in part by National Science Foundation Grant DCB8801873 (to M. T. H.). A portion of this work was presented at the FASEB meeting in Las Vegas, NV, May 1–5, 1988. The costs of publication of this article were defrayed in part by the payment of page charges. This article must therefore be hereby marked "*advertisement*" in accordance with 18 U.S.C. Section 1734 solely to indicate this fact.

‡ To whom correspondence should be addressed. Tel.: 505-646-3418.

[1] The abbreviations used are: CD site, metal-binding site in oncomodulin or parvalbumin flanked by the C and D helices; EF site, metal-binding site in parvalbumin flanked by the E and F helical regions; PBS, phosphate-buffered saline; Tween 20, polyoxyethylenesorbitan monolaurate; *tac* promoter, a hybrid promoter formed by fusion of the tryptophan and lactose promoters; PAGE, polyacrylamide gel electrophoresis, SDS, sodium dodecyl sulfate; D59E, site-specific variant of recombinant oncomodulin in which aspartate 59 has been replaced by glutamate; Y65F, site-specific variant of recombinant oncomodulin in which tyrosine 65 has been replaced by phenylalanine; MES, 2-(*N*-morpholino)ethanesulfonic acid; HEPES, 4-(2-hydroxyethyl)-1-piperazineethanesulfonic acid.

nucleotide-directed mutagenesis.

The potential importance of the -*X* ligand, the so-called "fifth ligand," in modulating the affinity and specificity of calcium-binding loops has been recognized for some years. Kretsinger (1) noted the invariant glutamate at this position in the CD- and EF-binding domains of the parvalbumins. More recently, Herzberg and James (21) discussed the presence of shorter side chains, aspartate or serine, at the equivalent position in all four domains of calmodulin and in the two regulatory domains of troponin C. The significance of their observation stems from the fact that, while the carboxyl of glutamate can coordinate directly to the bound metal ion, the oxygen atom(s) of the shorter side chains coordinate metal ions indirectly via a bound water molecule. Since the stabilities of metal-chelate complexes are determined in part by the extent of dehydration of the bound ion, the identity of the fifth ligand in a given binding domain could be crucial in determining the affinity and, hence, specificity of that domain.

Rat oncomodulin displays extensive sequence homology with rat parvalbumin. The aligned sequences are identical at 55 of 108 positions (22–24). Nevertheless, an aspartate residue occupies the fifth coordination position in the CD site of oncomodulin, the putative Ca^{2+}-specific site, whereas parvalbumin contains a glutamate at this position. Consistent with the hypothesis of Herzberg and James (21), it has been suggested (20) that this aspartyl side chain is too short to directly coordinate to the metal ion and must, therefore, be coordinated indirectly via a bridging water molecule. Work by Sykes and his colleagues (25, 26) on parvalbumin has clearly shown that the CD- and EF-binding domains of parvalbumin differ in their interactions with metal ions of different sizes. The EF site appears to be relatively flexible and will accommodate lanthanide ions of diverse size. On the other hand, the CD site is more rigid, more cryptand-like, exhibiting a marked preference for the larger lanthanide ions. Williams *et al.* (20) suggested that the substitution of aspartate for glutamate at position 59 of oncomodulin further increases the preference of the site for larger ions and accounts for much of the increased calcium specificity of the oncomodulin CD site. According to this hypothesis, binding of Mg^{2+} ion might be disfavored relative to calcium ion because the smaller ion would be less completely desolvated than Ca^{2+} when bound in this larger relatively rigid binding domain.

On the basis of these arguments, we chose to replace the aspartyl residue at position 59 of oncomodulin with a glutamate residue, the residue present in all parvalbumins examined to date, in order to determine whether a more parvalbumin-like site resulted. The $^7F_0 \rightarrow {}^5D_0$ Eu^{3+} excitation spectra[2] obtained with fully bound parvalbumin and oncomodulin are superficially similar (27); however, there are several important differences. We were particularly interested in learning whether the substitution of glutamate for aspartate at position 59 would afford a protein more closely resembling a parvalbumin.

In this paper, we describe the cloning and expression of oncomodulin, production of site-specific variants by oligonucleotide-directed mutagenesis, and characterization of the proteins using Eu^{3+} luminescence spectroscopy and Ca^{2+}-binding measurements.

[2] $^7F_0$ and $^5D_0$ are term symbols denoting the ground electronic state and first excited state, respectively, of the Eu^{3+} ion. $^7F_0 \rightarrow {}^5D_0$ indicates the electronic transition that occurs upon absorption of a photon of the appropriate energy.

EXPERIMENTAL PROCEDURES

Materials—Oligonucleotides, synthesized on a Beckman DNA synthesizer, were purified by electrophoresis through a 20% polyacrylamide gel containing 7.0 M urea in the presence of Tris-borate-EDTA buffer. The bands of lowest mobility were excised and extracted for use as primers in sequencing and oligonucleotide-directed mutagenesis and as end-labeled probes.

Europium sesquioxide (Eu_2O_3) was the generous gift of Molycorp, Inc. Solutions of $EuCl_3$ were prepared by dissolution of the sesquioxide in concentrated HCl, followed by removal of the excess HCl. They were standardized by titration with EDTA at pH 6.0 to a Xylenol Orange end point as described by Lyle and Rahman (28). All other chemicals were reagent grade or better.

Electrophoresis—Discontinuous SDS-PAGE was performed in 7.5–20% gradient gels using the Laemmli buffer system (29). Gels were silver-stained by the method of Morrissey (30). Urea gradient gel electrophoresis was performed as described by Creighton (31), and the gels were stained with a 1:5 dilution of Bio-Rad protein assay reagent. Agarose gel electrophoresis was performed as described in Maniatis *et al.* (32).

Immunochemistry—Polyclonal antibodies against rat oncomodulin were raised in a male New Zealand White rabbit by multiple subcutaneous injections (33) of tumor-derived oncomodulin emulsified with Ribi adjuvant (Ribi ImmunoChem Research, Inc., Hamilton, MT).

Electrophoretic transfer of proteins to nitrocellulose membranes was performed as described by Erickson *et al.* (34). Prior to use, the nitrocellulose replicas were blocked for 1–2 h at room temperature in 5% (w/v) nonfat dry milk in 50% (v/v) calf serum, 50% PBS. Primary and secondary antibodies were diluted into the same solution containing 0.05% (v/v) Tween 20 (35) in addition. Washes were performed with PBS containing 0.05% Tween 20 (PBS/Tween).

Expression of oncomodulin in *E. coli* was detected immunologically employing the method of Helfman *et al.* (36), probing first with an adsorbed preparation of rabbit anti-oncomodulin (final dilution 1:1000) and then with an affinity-purified preparation of ^{125}I-labeled goat anti-rabbit IgG (Du Pont-New England Nuclear). Antibodies directed against *E. coli* antigens were removed from the rabbit antiserum before use by adsorption with an *E. coli* lysate immobilized on Bio-Rad Affi-Gel 10.

Spectroscopy—UV absorption spectra were acquired on a Perkin-Elmer 320 UV-visible spectrophotometer. Eu^{3+} $^7F_0 \rightarrow {}^5D_0$ excitation spectra were acquired with the laser spectrofluorimeter described previously (27, 37), employing an emission wavelength of 618 nm. Spectral deconvolution and curve fitting were performed as described previously (27) employing the public procedure FITFUN, within the PROPHET computer resource sponsored by the Department of Research Resources of the National Institutes of Health.

Binding Measurements—Dissociation constants for Ca^{2+} at pH 7.4 were determined at room temperature (22 ± 1 °C) by the flow dialysis technique of Colowick and Womack (38), using a sample cell based on their design. A flow rate of 2.0 ml/min was maintained through the lower chamber by means of a Rainin peristaltic pump. The eluate was sampled 5 min after each addition of Ca^{2+}, and three 0.4-ml aliquots were counted in 5 ml of 3a70B scintillation mixture (Research Products, Inc.). 15 μCi of $^{45}CaCl_2$ (Du Pont-New England Nuclear, 31 mCi/mg of Ca^{2+}) was used per determination, and the protein concentration in the upper chamber was 100 μM. Depletion of $^{45}Ca^{2+}$ from the upper chamber during the course of the experiments, which lasted less than 2 h, was less than 5%. No correction was applied.

Bound metal ion was removed from our protein preparations by adding 2 eq of Eu^{3+} and then passing the resulting solution over a 1 × 18-cm column of EDTA-agarose (39) at a flow rate of 0.3–0.5 ml/min. The absence of a luminescence signal at 580 nm due to the $^7F_0 \rightarrow {}^5D_0$ transition indicated that removal of Eu^{3+} by this procedure was complete; and the residual Ca^{2+} content was <0.1 g atoms/mol of protein, as determined by flame atomic absorption employing a C_2H_2/N_2O flame. Buffers employed in binding or luminescence studies were likewise passed over an EDTA-agarose column, reducing the level of contaminating Ca^{2+} to less than 1 μM.

The binding data were fit to a parametric form of a two-site Scatchard equation,

$$r/[Ca^{2+}] = (1/K_{EF})/(1 + [Ca^{2+}]/K_{EF}) + (1/K_{CD})/(1 + [Ca^{2+}]/K_{CD}) \quad (1)$$

where r is the number of moles of Ca^{2+} bound per mol of protein and K_{EF} and K_{CD} represent the dissociation constants for the EF and CD

binding sites, respectively. This treatment assumes that there is no cooperative interaction between the sites. Evaluation of K_{EF} and K_{CD} was performed using FITFUN.

Mg^{2+} binding constants were determined by competition with the Ca^{2+} ion. For these experiments, 1.0 mM Mg^{2+} was included in both the upper chamber and in the buffer passed through the lower chamber. The stock Mg^{2+} solution was prepared by dissolution of purified magnesium metal with Ultrex® grade HCl (J. T. Baker Chemical Co.). In the presence of competing Mg^{2+} ion, the dissociation constant for Mg^{2+}, K_{Mg}, is related to the apparent dissociation constant for Ca^{2+}, $K_{Ca'}$, through the equation,

$$K_{Ca'} = K_{Ca}\{1 + [Mg^{2+}]/K_{Mg}\} \quad (2)$$

where K_{Ca} is the intrinsic dissociation constant for Ca^{2+}. In the calculation of K_{Mg}, the $[Mg^{2+}]$ was not corrected for binding at the other site. The resulting error in K_{Mg} is less than 10%.

RESULTS

Cloning of Rat Oncomodulin cDNA—Recombinant DNA manipulations were performed in accordance with National Institutes of Health guidelines. The monograph by Maniatis *et al.* (32) served as our primary resource for common procedures.

mRNA was isolated from monolayers of 5123tc (cultured in RPMI 1640 medium supplemented with 5% horse serum) by a minor modification of the procedure described in Maniatis *et al.* (32). Enrichment for poly(A^+) RNA was achieved by two cycles of binding and elution from oligo(dT)-cellulose. Double-stranded cDNA was synthesized from 10 μg of mRNA by the procedure of Gubler and Hoffman (40). After attaching *Cla*I linkers, the cDNA population was inserted into the *Cla*I site of Bluescript. Transformation of Library Efficiency® *E. coli* DH5α (Bethesda Research Laboratories) with 10 ng of the resulting preparation yielded approximately 90,000 recombinants, which were replica-plated onto nitrocellulose filters (Millipore) and screened sequentially with end-labeled oligonucleotides complementary to the 3′ and 5′ ends of the coding sequence (24).

Twenty-one colonies from a cDNA library of approximately 90,000 recombinants hybridized to a probe for the sequence immediately downstream from the COOH-terminal codon. This frequency suggests that the oncomodulin message corresponds to approximately 0.023% of the total hepatoma mRNA, substantially higher than the frequency reported by Gillen *et al.* (24). Of the 21 positive clones, 20 hybridized to a probe for the region immediately upstream from the start codon and presumably contained the entire oncomodulin coding sequence. Plasmid DNA was isolated from seven of the positive colonies, digested with *Cla*I, and analyzed by agarose gel electrophoresis. The insert size varied from 548 to 725 base pairs. The plasmid harboring the shortest insert, pRH4, was selected as the starting point for expression in *E. coli*. Sequence analysis revealed that, relative to the sequence reported by Gillen *et al.* (24), the pRH4 insert lacked 165 base pairs from the 3′ end but contained an additional 53 base pairs at the 5′ end of the gene.

Expression of Rat Oncomodulin Coding Sequence—The strategy employed for expressing oncomodulin in *E. coli* is diagrammed in Fig. 1. The vector chosen for expression was pKK223-3 (Pharmacia LKB Biotechnology Inc.) Prior to inserting the oncomodulin sequence into pKK223-3, the unique *Eco*RI site in the vector was replaced by a *Kpn*I site using linkers, affording pKK223-3.2. A sample of this plasmid was then prepared for cloning by linearizing with *Hin*dIII and filling in the 5′ overhangs with the Klenow fragment of DNA polymerase. The oncomodulin cDNA insert was liberated from pRH4 as a *Bam*HI-*Sal*I fragment, likewise filled in with Klenow, electrophoretically purified, and ligated into the

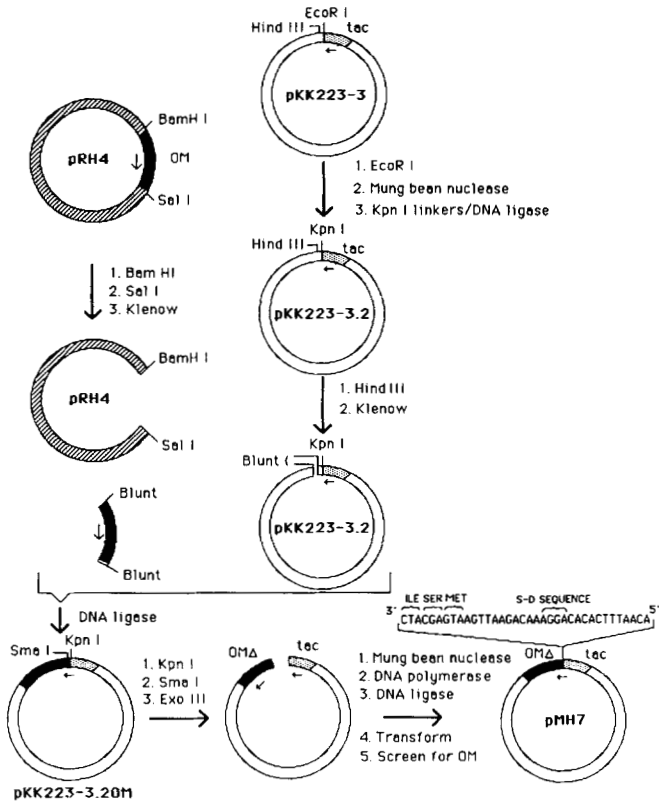

FIG. 1. **Strategy employed for achieving expression of oncomodulin (*OM*) in *E. coli*.**

blunt-ended vector. Following transformation of *E. coli* DH5α, recombinants were identified by colony blot hybridization using an end-labeled probe for the 5′ end of the cDNA. The desired orientation was verified by restriction analysis.

The resulting construction, labeled pKK223-3.2OM, was prepared for unidirectional deletion with exonuclease III by sequential treatment with *Kpn*I and *Sma*I. The 3′ overhang generated by *Kpn*I protected the promoter region from deletion, since ExoIII will only initiate digestion at blunt ends or 5′ overhangs. Deletions were performed according to instructions supplied by Stratagene with the Bluescript vector. Following recircularization with DNA ligase, the preparation was used to transform Library Efficiency® *E. coli* DH5α.

Approximately 20,000 colonies were screened for oncomodulin expression by colony Western blot (36). Those affording the 11 strongest signals were chosen for further characterization and labeled pMH1 through pMH11. Liquid cultures of all 11 clones were harvested in midlog phase, and crude extracts were prepared using an equal number of cells from each culture. Serial dilutions of the extracts were spotted onto nitrocellulose, probed with adsorbed rabbit anti-oncomodulin, and ^{125}I-goat anti-rabbit IgG and autoradiographed. pMH4 and pMH11 displayed the highest levels of expression. Oncomodulin production by pMH6 and pMH7, the next highest overproducers, was lower by a factor of approximately 2.

Although the recombinant oncomodulin expressed by pMH6 and pMH7 co-migrates with tumor-derived oncomodulin during nondenaturing PAGE, the majority of the oncomodulin expressed in pMH4 and pMH11 had a lower relative mobility (Fig. 2). However, all four proteins co-migrate during SDS-PAGE, and all four plasmids have the same coding sequence reported by Gillen *et al.* (24). Until we understand the origin of the altered electrophoretic mobility, we are using

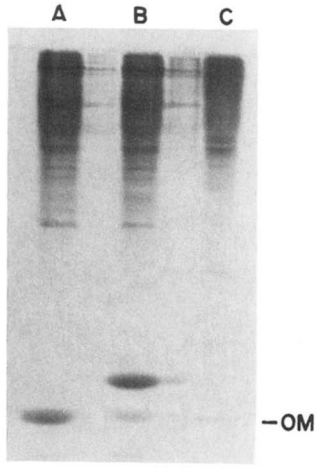

FIG. 2. **Nondenaturing polyacrylamide gel electrophoresis of crude extracts of pMH4 and pMH7.** Late log phase cultures of *E. coli* DH5α harboring either pMH4 or pMH7 were harvested, resuspended in approximately 4 volumes of Buffer A (41) and lysed by sonication following lysozyme treatment. After centrifuging out the cell debris, samples of the lysates were subjected to discontinuous polyacrylamide gel electrophoresis, as described under "Experimental Procedures." *Lane A*, pMH7; *lane B*, pMH11; *lane C*, extract of Morris hepatoma 5123tc. The band corresponding to tumor-derived oncomodulin (*OM*) is indicated.

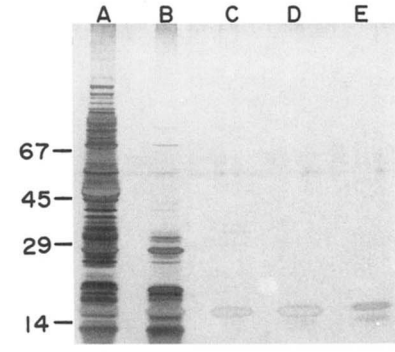

FIG. 3. **Purification of recombinant oncomodulin as monitored by SDS-PAGE.** Samples from the various stages of purification were subjected to polyacrylamide gel electrophoresis on a 7.5–20% gradient gel in the presence of SDS and 2-mercaptoethanol. Proteins were visualized by silver staining. *Lane A*, crude lysate; *lane B*, heat-treated lysate; *lane C*, pooled fractions from the DEAE-cellulose column; *lane D*, pooled fractions from the Sephadex G-75 column; *lane E*, tumor-derived oncomodulin.

pMH7 as our expression vector for wild-type recombinant oncomodulin.

pMH6 and pMH7, which produce ≈3% of the total protein as oncomodulin, were found to have 12 and 18 nucleotides, respectively, between the Shine-Dalgarno sequence and the start codon. pMH4, which produces just over twice as much of the recombinant protein, has 16 nucleotides between the ribosome-binding site and the start codon. It appears, then, that the optimal separation is approximately 16 nucleotides.

Purification of Recombinant Oncomodulin—E. coli DH5α harboring either pMH7 or a site-directed variant thereof was grown to late log phase at 37 °C with continuous shaking in 1-liter cultures of LB broth containing 50 μg/ml ampicillin. In DH5α, maximal expression of recombinant oncomodulin was observed even in the absence of isopropyl-1-thio-β-D-glucopyranoside. Each liter of culture yielded 3.5–4.0 g of cell paste, which was collected by centrifugation, washed once with PBS, and stored at −80 °C prior to use.

Bacterial cell lysis was achieved by treatment with lysozyme (0.5 mg/g of cell paste) and passage through a French pressure cell. Employing a modification of the procedure by MacManus (41), the preparation was subjected to heat treatment at 80 °C, ion exchange chromatography on DEAE-Sepharose (Pharmacia), and gel filtration through Sephadex G-75 (Pharmacia). The progress of an isolation of recombinant oncomodulin from pMH7, as monitored by SDS-PAGE, is presented in Fig. 3. The material collected from the gel filtration column is highly purified. Only a single minor contaminant is visible (running just ahead of the major band) on an overloaded silver-stained SDS gel.

Protein concentrations were determined spectrophotometrically for solutions of recombinant oncomodulin. An extinction coefficient at 275 nm of 3650 M^{-1} cm^{-1} was determined for the wild-type protein on the basis of careful and repeated titration of the protein with Eu^{3+}. Extinction coefficients were obtained for the site-specific variants discussed below with the Bio-Rad protein assay, employing solutions of known absorbance and using wild-type recombinant oncomodulin of known concentration as a standard.

Site-specific Mutagenesis of Rat Oncomodulin—The Bluescript cloning vector contains the intergenic region of bacteriophage M13, thus permitting production of single-stranded plasmid in *E. coli* infected with a helper phage (VCS-M13, purchased from Stratagene). We utilized this feature of Bluescript to produce the coding strand of pRH4. To increase the frequency of the mutant phenotype, we employed the strategy of Kunkel (42, 43), producing our single-stranded DNA in a host that was deficient in dUTPase (*dut*$^-$) and uracil-*N*-glycosylase (*ung*$^-$). To the resultant uracil-containing single-stranded template, we annealed a 5′-phosphorylated oligonucleotide bearing a single nucleotide mismatch responsible for either the mutation of aspartate 59 to glutamate or tyrosine 65 to phenylalanine. Double-stranded circular DNA, produced by extension with T4 DNA polymerase and recircularization with T4 DNA ligase, was used to transform *E. coli* DH5α.

Recombinants harboring the desired mutation were detected by the method of Norris *et al.* (44). Twenty colonies selected at random were grown in 1.5-ml cultures, harvested in late log phase, and lysed by the method of Holmes and Quigley (45). NaOH and NaCl were added to the lysates to denature the plasmid DNA, and samples of the six lysates were spotted onto three nitrocellulose filters. Following neutralization and wash steps, the filters were probed with the approriate end-labeled mutant oligonucleotide for 4 h at 30 °C. After a brief rinse at room temperature, single 5-min washes were then performed at T_m − 12 °C, T_m − 6 °C, or T_m in 6 × SSC, with each filter being treated at a different temperature. The melting temperature T_m was estimated from the composition of the particular oligonucleotide using the formula given by Maniatis *et al.* (32). Autoradiographic signals which persisted at the higher stringencies were presumed to originate from colonies bearing the mutant genotype. Plasmid DNA was isolated from these colonies and sequenced to verify the presence of the altered genotype. Mutants bearing either a tyrosine → phenylalanine mutation at position 65 (pRH12) or an aspartate → glutamate substitution at position 59 (pRH13) were isolated in this manner.

Expression of the mutant alleles required that we shuttle the altered sequence from Bluescript into our expression plasmid, pMH7. To accomplish this, we made use of unique *Pst*I and *Eco*RI sites at codons 16 and 101, respectively, in the oncomodulin coding sequence (24). Thus, we treated pRH12 and pRH13 sequentially with *Pst*I and *Eco*RI, isolated the appropriate fragments from a 1.4% agarose gel, and cloned them into pMH7 that had likewise been treated with *Pst*I and

*Eco*RI and gel purified. The resultant plasmids were sequenced to verify the presence of one, and only one, nucleotide modification. The recombinant protein containing the tyrosine → phenylalanine substitution is subsequently denoted as Y65F, while the protein containing the aspartate → glutamate substitution is referred to as D59E.

Characterization of the Mutant Oncomodulins—The recombinant oncomodulins we have isolated (wild-type and mutations alike) behave similarly to the tumor-derived protein during purification, withstanding heat treatment at 80–83 °C for 5 min and fractionating similarly on ion exchange and gel filtration. Moreover, the mobilities of all three recombinant proteins under denaturing or nondenaturing conditions are indistinguishable from the tumor-derived protein. These observations imply: 1) that the structure and stability of recombinant oncomodulin must be very similar to those of the tumor-derived protein; and 2) that the two site-specific modifications we have introduced have not significantly diminished the stability of the polypeptide.

The latter conclusion is substantiated by urea gradient gel electrophoresis. This technique employs electrophoretic mobility as a conformational probe (31). In general, the mobility of proteins through a polyacrylamide matrix decreases upon denaturation, since the unfolded form has a greater volume. Thus, if protein is loaded across the top of a polyacrylamide gel containing a horizontal gradient of urea and subjected to electrophoresis, a wave in the mobility is observed (Fig. 4). If the observed mobility is plotted as a function of urea concentration in the gel, the concentration of urea required for denaturation (the midpoint) can be determined. The values obtained for wild-type oncomodulin and the D59E and Y65 variants were 3.5, 3.6, and 3.4 M, respectively, suggesting that the three proteins have similar conformational stabilities. Interestingly, the protein bands split in the transition region. This phenomenon suggests (31) the presence of two distinct, but electrophoretically indistinguishable, native conformations of oncomodulin that do not interconvert on the time scale of the electrophoresis (270 min) at 4 °C. The two forms might represent, for example, *cis* and *trans* conformations of the polypeptide backbone immediately preceding either of the proline residues at positions 21 and 26. At higher temperatures, the discrete bands in the transition zone are replaced by a broad smear, indicating more rapid interconversion of conformers.

Eu^{3+} Luminescence Properties of the Recombinant Oncomodulins—The utility of Eu^{3+} as a spectroscopic probe derives in part from its ability to undergo an electronic transition near 580 nm involving the $^7F_0$ ground state and the $^5D_0$ excited state (46). This transition is nondegenerate, so that each distinct Eu^{3+} species in solution (or each binding site in a multisite protein) should give rise to a single peak having a typical line width on the order of 5 Å. Since the $^7F_0 \rightarrow {}^5D_0$ transition is highly forbidden ($\epsilon \approx 0.01\ M^{-1}\ cm^{-1}$), it can only be studied in dilute solutions of biological materials by employing an intense laser source and measuring the luminescence (at 618 nm) that accompanies return of the ion to the ground state. The display of luminescence intensity *versus* the wavelength of absorbed light is referred to as the Eu^{3+} $^7F_0 \rightarrow {}^5D_0$ excitation spectrum. This transition has been used to study such calcium-binding proteins as thermolysin (47), troponin C (48), calmodulin (49, 50), phospholipase A (51), parvalbumin (27, 52–55) and oncomodulin (27, 55).

The $^7F_0 \rightarrow {}^5D_0$ spectrum of fully bound recombinant oncomodulin is presented in Fig. 5*B*. In most respects, it mimics that observed with the tumor-derived protein (Fig. 5*A*). At pH 5.0, it is dominated by a slightly asymmetric peak at 5795 Å. Although this "low pH" spectrum arises from Eu^{3+} ions bound at both the CD and EF sites, only a single peak is observed, presumably because the two spectral contributions are nearly coincident. In further analogy to the tumor-derived protein, the peak at 5795 Å is replaced at higher pH values

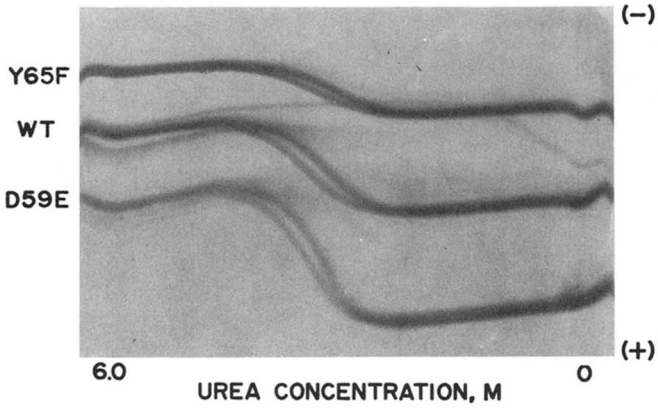

FIG. 4. **Urea gradient gel electrophoresis on recombinant oncomodulin and the D59E and Y65F site-specific variants.** The polyacrylamide gel, which was cast as described by Creighton (31), incorporated a 0–6.0 M gradient of urea and a 16–12% gradient of acrylamide. The purpose of the reverse acrylamide gradient was to compensate for variation in mobility resulting from increased viscosity at higher urea concentrations. 0.050 M MES, pH 6.5, containing 1 mM EDTA, served as the gel and reservoir buffer. The EDTA was included to ensure that the proteins would be in their apo forms. The three proteins were loaded at 2-h intervals. Electrophoresis was performed at 300 V at 4 °C. The gel was stained with Bio-Rad protein assay reagent.

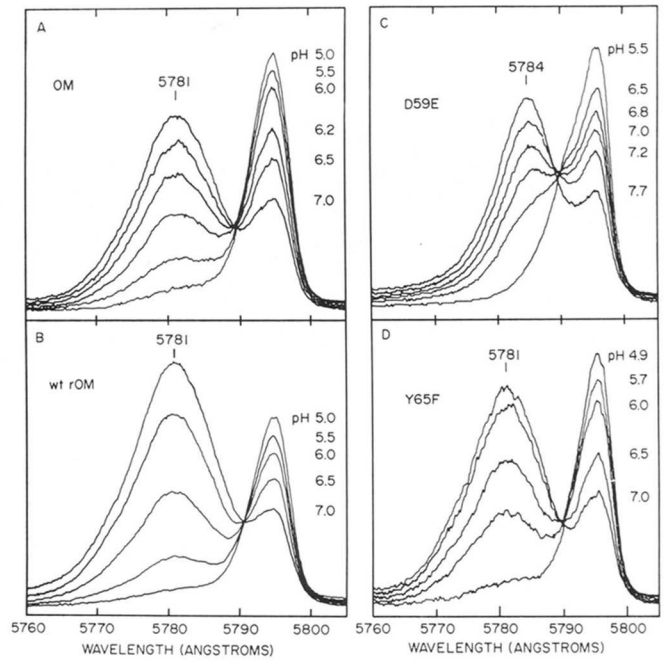

FIG. 5. **pH Dependence of Eu^{3+} $^7F_0 \rightarrow {}^5D_0$ excitation spectra of oncomodulin (*OM*), recombinant oncomodulin (*rOM*), D59E, and Y65F.** Eu^{3+} ion was added to 50 μM solutions of the apoproteins in 0.15 M NaCl, 0.025 M MES, pH 6.5, to afford Eu^{3+}: protein ratios of 2.0. Dilute HCl was then added to lower the pH to approximately 5.0, and the $^7F_0 \rightarrow {}^5D_0$ spectrum was acquired. The pH of the solution was then adjusted upward with dilute NaOH, acquiring the Eu^{3+} spectrum after each addition. *Panel A* displays the behavior of the spectrum obtained with tumor-derived rat oncomodulin; *panel B*, the behavior of the wild-type (*wt*) recombinant oncomodulin; *panel C*, the behavior of the site-specific variant D59E; and *panel D*, the behavior of Y65F.

by a broad intense spectrum centered at 5781 Å. When the intensity at 5781 Å is plotted *versus* pH (Fig. 8), a pK_a for this spectral transition of 6.0 ± 0.1 is extracted. This value is lower than the pK_a determined for the tumor preparations (6.3 ± 0.1) and, together with the somewhat greater intensity of the high pH spectrum, may signal an altered conformation at the NH_2 terminus of the recombinant protein.

Substitution of a glutamyl residue for the aspartyl residue normally present at position 59 of oncomodulin, via site-specific mutagenesis, alters the Eu^{3+} $^7F_0 \rightarrow {}^5D_0$ spectrum in several respects. Selected spectra from a Eu^{3+} titration of apoD59E, performed at pH 5.0, are presented in Fig. 6. At low ratios of Eu^{3+}:protein, a single sharp peak is present, centered at 5795 Å. As the titration proceeds, however, a prominent shoulder appears at 5791 Å. Thus, the two metal ion-binding sites in D59E are filled sequentially by Eu^{3+}, with occupation of the EF site occurring first. This behavior was noted previously with the tumor-derived protein (27) and occurs with the wild-type recombinant protein as well (data not shown).

For purposes of comparison, the spectrum of the D59E mutant protein containing two equivalents of Eu^{3+} at pH 5.0 is presented in Fig. 7, together with the corresponding spectra for the wild-type recombinant oncomodulin and rat and pike parvalbumins. The D59E spectrum displays a shift in the position of the CD signal to lower wavelength relative to the spectrum of the wild-type protein. In fact, the location of the CD signal, at 5791 Å, is quite similar to that observed for the CD site in pike parvalbumin (37). The intensities and line widths differ, however, accounting for the somewhat different overall appearance of the spectrum.

The $^7F_0 \rightarrow {}^5D_0$ spectrum of the fully bound D59E variant is displayed as a function of pH in Fig. 5*C*. Qualitatively, the behavior resembles that observed with the wild-type oncomodulin. However, there are two noteworthy differences. The position of the high-pH peak observed with the mutant protein is shifted to higher wavelength. As observed with pike and rat parvalbumins, the spectrum appears at 5784 Å for the mutant protein rather than 5781 Å, as observed with tumor-derived and wild-type recombinant oncomodulins. Furthermore, the pH dependence is altered, with the spectral transition now occurring at substantially higher pH. The pK_a value

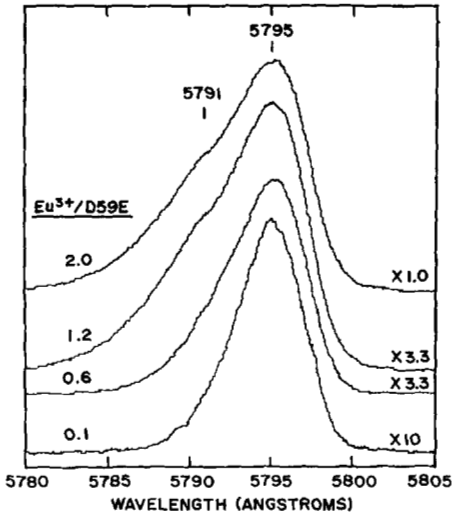

FIG. 6. **Sequential occupation of EF- and CD-binding domains of D59E by Eu^{3+}.** A 50 μM solution of apoD59E was titrated with Eu^{3+} at pH 5.0 in 0.15 M NaCl, 0.025 M MES. The appearance of the $^7F_0 \rightarrow {}^5D_0$ spectrum is displayed above for several Eu^{3+}:protein ratios. The relative gain is noted to the right of each spectrum.

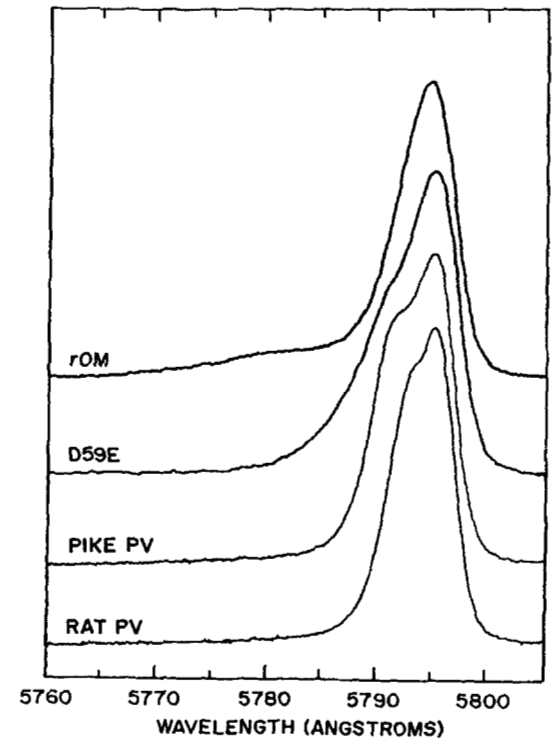

FIG. 7. **Low pH $^7F_0 \rightarrow {}^5D_0$ spectra of recombinant oncomodulin (*rOM*), D59E, pike parvalbumin, and rat parvalbumin.** Spectra were acquired on 50 μM solutions of the proteins containing 2 molar eq of Eu^{3+} ion. In each case, the solution contained 0.15 M NaCl and 0.025 M MES, pH 5.0.

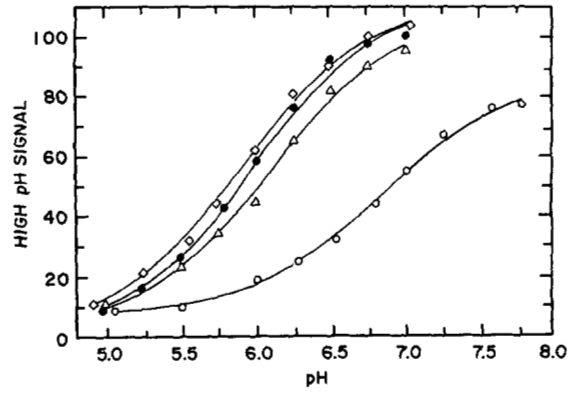

FIG. 8. **pH-dependent behavior of recombinant oncomodulin and site-specific variants.** The intensity of the high-pH signal is displayed above as a function of pH for tumor-derived rat oncomodulin (△), wild-type recombinant oncomodulin (●), Y65F (◇), and D59E (○). pH titrations were performed as described in the legend to Fig. 7.

determined for the D59E mutation is 6.8 (Fig. 8), as compared with 6.0 for the wild-type protein. Since the corresponding pK_a value for a parvalbumin-type site is ≈8.2, the observed shift is in the expected direction for a mutation producing a more parvalbumin-like CD-binding domain.

The pH dependence of the $^7F_0 \rightarrow {}^5D_0$ spectrum observed with the Y65F mutant, in which phenylalanine replaces tyrosine at position 65, is presented in Fig. 5*D*. It is important to note that the appearance of the low pH spectrum, peak position of the high pH spectrum, and the pK_a determined for the pH-dependent spectral transition (pK_a = 5.9) are very similar to those observed in the wild-type spectrum. Thus, the spectral alterations that accompany replacement of aspartate 59 with

glutamate do not appear to be nonspecific effects resulting from indiscriminate substitution of residues near the CD-binding domain.

Affinities of Recombinant Oncomodulin and D59E for Ca^{2+} and Mg^{2+}—The binding of Ca^{2+} to aporecombinant oncomodulin was studied in 0.15 M NaCl, 0.025 M HEPES, pH 7.4, by flow dialysis, as described under "Experimental Procedures." When subjected to Scatchard analysis, the data afforded distinctly biphasic plots (Fig. 9 *left*, ●). This behavior suggests that the two binding sites of oncomodulin have very different affinities for Ca^{2+}, consistent with their distinct ion binding specificities (18, 19). Values for K_{Ca} at the CD and EF sites were extracted by fitting the binding data to a two-site Scatchard model (Equation 1). The results for three separate determinations are listed in Table I. The mean values are 0.78 ± 0.07 μM for the CD site and 42 ± 5 nM for the EF site. This result is in marked contrast to parvalbumin, where both binding sites have the same specificity and behave equivalently during titrations with Ca^{2+}, displaying dissociation constants of 10^{-8}–10^{-9} M (8, 56, 57).

In order to estimate values for K_{Mg} at the two binding sites, calcium-binding measurements were performed in the presence of 1.0 mM Mg^{2+} (Fig. 9 *left*, ○). Results from three experiments are also presented in Table I. Under these conditions, the observed dissociation constants, $K_{Ca'}$, are related to the true dissociation constants, K_{Ca} and K_{Mg}, as indicated in Equation 2 under "Experimental Procedures." The mean values for K_{Ca} and $K_{Ca'}$ were used in the calculation of K_{Mg}. Values for K_{Mg} of 3 and 0.16 mM were extracted for the CD and EF sites, respectively, of wild-type recombinant oncomodulin.

When apoD59E is titrated with Ca^{2+}, the resulting Scatchard plot (Fig. 9*B*, ●) is qualitatively similar to that obtained with the wild-type protein. Binding constants determined from three separate experiments are displayed in Table I. The average values of K_{Ca} determined for the CD and EF sites are 0.55 ± 0.08 μM and 42 ± 7 nM, respectively. Thus, the substitution at residue 59 appears to have caused a slight increase in the affinity of the CD site for Ca^{2+} while leaving the binding constant for the EF site unchanged. Values of $K_{Ca'}$ determined in the presence of 1.0 mM Mg^{2+} (Fig. 9*B*, ○) are consistent with magnesium dissociation constants (K_{Mg}) of 1 and 0.18 mM for the CD and EF sites, respectively. It is worth emphasizing that the $K_{Ca'}$ values measured for the CD sites in the wild-type and mutant proteins span a rather broad range (±30%), introducing substantial uncertainty into the K_{Mg} values. The significance of the observed differences in K_{Mg} for the two proteins should be interpreted in this light.

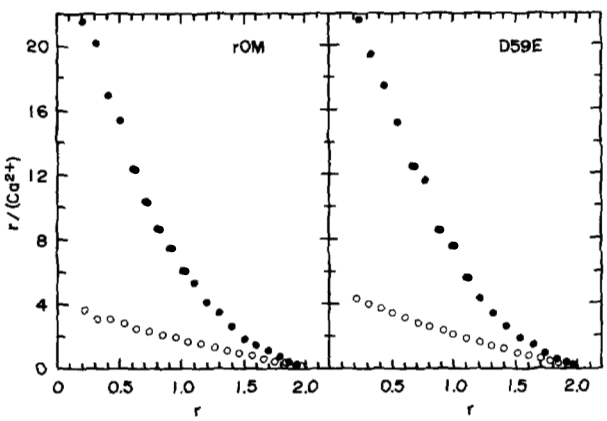

FIG. 9. **Binding of Ca^{2+} to recombinant oncomodulin (*rOM*) and D59E in the presence and absence of Mg^{2+}.** Flow dialysis measurements were performed as described under "Experimental Procedures," and the data is displayed in Scatchard format as $r/[Ca^{2+}]$ *versus* r, where r is the fraction of total Ca^{2+} ion bound and $[Ca^{2+}]$ is the free Ca^{2+} concentration. Measurements were performed in the presence (○) and absence (●) of 1.0 mM Mg^{2+}. Data for the wild-type recombinant protein is presented in the *left panel*, while the corresponding data for the D59E variant is displayed on the *right*.

TABLE I

Ca^{2+} and Mg^{2+} dissociation constants determined for rOM and D59E

Conditions are specified under "Experimental Procedures."

Protein	Site	K_{Ca}	K_{Ca} average	$K_{Ca'}$[a]	$K_{Ca'}$ average	K_{Mg}[b]
		μM	μM	μM	μM	mM
rOM	CD	0.71		1.0		
		0.82	0.78	1.3	1.0	3
		0.80		0.8		
	EF	0.040		0.32		
		0.047	0.042	0.27	0.31	0.16
		0.038		0.33		
D59E	CD	0.47		0.9		
		0.55	0.55	1.4	1.2	1
		0.63		1.2		
	EF	0.040		0.26		
		0.036	0.042	0.28	0.28	0.18
		0.049		0.29		

[a] Measured in the presence of 1.0×10^{-3} M Mg^{2+}.

[b] This number was calculated from Equation 2 (see "Experimental Procedures") using the mean values for K_{Ca} and $K_{Ca'}$.

DISCUSSION

Careful inspection of the calcium-binding loops found in intracellular calcium-binding proteins reveals certain commonalities. Each site contains six ligands arranged in a pseudo-octahedral configuration; four or five of the six are side chain oxygen atoms, while a peptide oxygen is coordinated at the $-Y$ position (2). In general, three or four of the liganding atoms are ionic oxygens from carboxylate groups, the remainder being neutral oxygen species furnished by serine, threonine, asparagine, or water. Certain domains have affinity for both Ca^{2+} and Mg^{2+} under physiological conditions, while others have affinity only for Ca^{2+}. However, despite a knowledge of the primary structures of numerous calcium-binding proteins, the factors which determine the binding specificity of calcium-binding sites have yet to be pinpointed. Apparently, neither the number of coordinating carboxylates nor the net charge in the binding loop is the sole determinant of specificity (1). It is entirely possible that residues outside of the binding loop *per se*, in the flanking helical regions, are critical determinants of specificity. Reid *et al.* (58), for example, have found that calcium-binding loops themselves have marginal affinity for calcium in aqueous solution and that the affinity is increased markedly by inclusion of both flanking helical elements. Moreover, the large decrease in affinity for Ca^{2+} which accompanies separation of the parvalbumin calcium-binding domains by limited proteolysis argues that domain-domain interactions might even be critical determinants of ion-binding properties (59).

The parvalbumins contain two high affinity calcium-binding domains, both of which fall into the Ca^{2+}/Mg^{2+} category (1). Oncomodulin, on the other hand, has been diagnosed as containing a single Ca^{2+}/Mg^{2+} site (the EF site) and a single Ca^{2+}-specific site (the CD site), despite extensive sequence homology with parvalbumin (18–20). We reasoned that systematic replacement of the parvalbumin codon for the oncomodulin codon at points of nonidentity in the CD binding domain might suggest which residues are critical for calcium specificity. In assessing the consequences of these substitu-

tions, we intend to use spectroscopic measurements with lanthanide ions as well as traditional metal ion-binding studies.

Lanthanide ions have proven to be useful probes of calcium-binding systems (60). Like Ca^{2+}, all have a preference for oxygen-containing ligands, high coordination numbers, and a tolerance for irregular coordination geometry. Additionally, those in the middle of the series have ionic radii similar to Ca^{2+}. Consequently, lanthanide ions readily substitute for Ca^{2+} in many calcium-binding proteins. In contrast to calcium ion, however, the lanthanides are amenable to study by a variety of spectroscopic techniques (60). We have found the luminescent lanthanide ions, Eu^{3+} and Tb^{3+}, to be particularly useful in studying several calcium-binding proteins, including parvalbumin and oncomodulin.

Generalizing from our studies of pike and rat parvalbumins (27, 37), we would conclude that the Eu^{3+} $^7F_0 \rightarrow {}^5D_0$ spectrum of a parvalbumin has three characteristic properties. 1) At low pH, the spectrum consists of a partially resolved doublet centered near 5795 Å; 2) at high pH, the spectrum consists of a broad intense peak centered at 5784 Å; and 3) the pK_a governing the interconversion of the two spectra is ≈8.2. We believe these features are diagnostic for a parvalbumin-like Ca^{2+}/Mg^{2+} site. Although there may be exceptions to these rules, they nonetheless provide a foundation for comparison of parvalbumin and oncomodulin from rat.

Until recently, our investigation of lanthanide-oncomodulin complexes had been hampered by the difficulty and expense involved in obtaining sufficient material for experimentation. Fortunately, the cloning and expression of the protein in *E. coli* has eliminated that obstacle; it is now possible to isolate 50–100 mg of highly purified recombinant oncomodulin with little difficulty, which has facilitated an examination of the recombinant protein in some detail by Eu^{3+} $^7F_0 \rightarrow {}^5D_0$ excitation spectroscopy.

In most respects, the spectral behavior of the recombinant protein mirrors that of the tumor-derived protein. The spectra observed with the fully bound proteins are both pH-dependent. Furthermore, the spectra obtained at the pH extremes are highly similar. However, the proteins appear to differ slightly with regard to the pH at which they undergo the pH-dependent spectral transition. Tumor-derived oncomodulin exhibits a pK_a for the transition of 6.3, whereas the wild-type recombinant protein exhibits a pK_a of 6.0. Furthermore, the intensity of the high-pH spectrum of recombinant protein is somewhat greater than that observed with tumor-derived oncomodulin. These spectroscopic differences may stem from structural differences at the NH_2 termini. The NH_2 terminus of the tumor-derived protein is *N*-acetylserine, whereas the NH_2-terminal residue of the recombinant preparations is either a serine, methionine, *N*-formylmethionine, or possibly a mixture of the three species.

Although superficially similar, the $^7F_0 \rightarrow {}^5D_0$ spectra arising from the CD-binding domains of rat oncomodulin and rat parvalbumin differ significantly in three respects. Whereas the features arising from the CD and EF sites are resolved in the parvalbumin spectrum at pH 5.0, the spectrum of fully bound oncomodulin exhibits a single peak. Moreover, the CD domain spectrum of parvalbumin undergoes a pH-dependent spectral transition with a pK_a = 8.2, whereas the CD site of oncomodulin undergoes an analogous transition at substantially lower pH values: pK_a = 6.3 for the tumor-derived oncomodulin, 6.0 for the recombinant protein. Additionally, the high pH spectrum assigned to the CD site of parvalbumin is centered at 5784 Å, while that assigned to the CD site of oncomodulin falls at 5781 Å. It was our hope in embarking upon a program of site-directed mutagenesis that we would be able to identify critical nonidentities in the two proteins responsible for these spectral differences and, furthermore, that these nonidentities would underlie the differing specificities of the two sites.

Oligonucleotide-directed mutagenesis, employing the strategy of Kunkel (42, 43) and screening method of Norris *et al.* (44), enabled us to produce two site-specific variants of oncomodulin with relatively little difficulty. We chose the aspartate to glutamate substitution at position 59 of oncomodulin as a starting point because cogent arguments by several investigators had indicated that the identity of the residue at this position was likely to be an important determinant of specificity (1, 20, 21). The consequences of this particular mutation were quite striking. To reiterate, substitution of glutamate for aspartate at position 59 of oncomodulin; 1) shifts the low-pH spectrum of the CD site to lower wavelength; 2) raises the pK_a for pH-dependent spectral transition undergone by the CD site; and 3) shifts the center of the CD high-pH spectrum from 5781 to 5784 Å. Each of these changes is in the direction expected for a more parvalbumin-like binding domain.

In contrast to the D59E mutant, replacement of tyrosine 65 by phenylalanine has very minor effects on the $^7F_0 \rightarrow {}^5D_0$ spectral characteristics of the oncomodulin CD site. This result gives us some confidence that the consequences of substituting glutamate for aspartate at position 59 are, in fact, highly specific effects and not merely the result of a general perturbation of the CD site structure. Although we anticipated that neither of these substitutions would cause disruption of the global structure of the protein, several observations support this hypothesis. The three recombinant proteins that we have examined, wild-type and mutant proteins alike, behave identically during purification, withstanding heating at 80 °C for 5 min. In addition. they exhibit virtually identical electrophoretic mobilities under denaturing and nondenaturing conditions. Moreover, all three proteins exhibit the same midpoint for the denaturation, 3.5 ± 0.1 M, upon urea-gradient gel electrophoresis, suggesting that the structure of the protein has been perturbed minimally by the single amino acid substitutions.

Based on results obtained with a series of model Eu^{3+} complexes, Albin and Horrocks (61) have proposed that the net charge of the Eu^{3+} complex is a primary determinant of peak position, with the transition being shifted to higher wavelength by ligands of increasingly negative charge. We would predict, then, that substitution of glutamate for aspartate at position 59 would bring the negatively charged carboxylate group into closer proximity to the bound Eu^{3+}, shifting the spectrum to higher wavelength. In fact, the observed shift in the position of the CD peak from ≈5795 to 5791 Å upon substitution of glutamate for aspartate is in the opposite direction. Interestingly, although the peak position for the low-pH CD spectrum is shifted to lower wavelength by the mutation, the center of the high-pH spectrum is shifted to higher wavelength (from 5781 to 5784 Å). At present, we lack an explanation for the opposing behaviors of the low- and high-pH spectra. However, the results certainly suggest that, at least with respect to protein complexes of Eu^{3+}, factors besides ligand charge are important determinants of peak position.

The pH-dependent spectral transition observed with oncomodulin and parvalbumin has been attributed to hydrolysis of a water molecule coordinated to the protein-bound Eu^{3+} ion (27, 37, 55). If this explanation is correct, then the pK_a for the transition should be sensitive to the net charge of the

metal-protein complex; the more positive the charge, the more highly polarized the bound water molecule and the lower the pH required for hydrolysis. Assuming that the coordination of the trivalent lanthanide precisely mimics that of Ca^{2+}, the effect of the D59E mutation on the pK_a for this transition is consistent with this explanation. The glutamyl carboxyl in the mutant at position 59 is presumably coordinated directly to the Eu^{3+} ion, whereas the aspartyl carboxyl in the wild-type protein is probably bound through a bridging water molecule (21). Thus, the net charge of the Eu^{3+}-CD site complex should be fractionally less positive for the D59E mutant than for the wild-type protein. Accordingly, we observe a higher pK_a for the putative hydrolysis.

We have also conducted a preliminary examination of the Ca^{2+} and Mg^{2+} binding properties of recombinant oncomodulin and the D59E site-specific variant. The results obtained with the wild-type protein offer further testimony to the nonequivalence of parvalbumin and oncomodulin. In Ca^{2+} binding studies conducted on various parvalbumins, the CD and EF binding sites are indistinguishable. The reported dissociation constants for Ca^{2+} range from 0.37 nM for carp (pI = 4.25) parvalbumin (57) to between 2 and 8 nM for frog, hake, and rabbit parvalbumins (8). The binding constants for Ca^{2+} reported for rat parvalbumin are 1–2 nM (62). By contrast, the two binding sites in oncomodulin exhibit distinctly different affinities for Ca^{2+}. K_{Ca} for the EF site is estimated at 42 nM, while $K_{Mg} = 0.16$ mM. The values obtained for the CD site of oncomodulin, on the other hand, are more than an order of magnitude greater: $K_{Ca} = 0.78$ μM and $K_{Mg} = 3$ mM. Interestingly, these values are quite similar to those determined by Rinaldi *et al.* (62) for another parvalbumin-like protein (distinct from oncomodulin) isolated from rat skin.

Ca^{2+}/Mg^{2+} sites and Ca^{2+}-specific sites differ markedly in their affinities for Ca^{2+} and Mg^{2+} (8, 9, 63). K_{Ca} is $< 10^{-7}$ M for a typical Ca^{2+}/Mg^{2+} binding site and 10^{-6}–10^{-7} M for a Ca^{2+}-specific site. K_{Mg} is $\leq 10^{-4}$ M for a Ca^{2+}/Mg^{2+} site and $>10^{-3}$ M for a Ca^{2+}-specific site. By these criteria, the EF site of oncomodulin clearly belongs to the Ca^{2+}/Mg^{2+} class, while the CD site falls into the Ca^{2+}-specific category. Thus, our binding data substantiate the claims made by MacManus and colleagues (18, 19) for the calcium-specific nature of the oncomodulin CD site.

The alterations in binding affinity that accompany the substitution of glutamate for aspartate at position 59 are not striking. There appears to be a perceptible increase in the affinity of the CD site for Ca^{2+}; K_{Ca} decreases from 0.78 to 0.55 μM. The replacement also appears to increase the affinity of the site for Mg^{2+}. The K_{Mg} calculated for the D59E site-specific variant is 1 mM, as compared with 3 mM for the wild-type protein. It should be noted, however, that these values of K_{Mg} are accompanied by a significant degree of uncertainty.

Judging from our binding data, the consequences of the D59E mutation appear to be confined to the CD binding domain. Replacement of Asp-59 by glutamate had no apparent influence on the affinity of the EF domain for either Ca^{2+} or Mg^{2+}; $K_{Ca} = 42$ nM for the EF sites in both wild-type recombinant oncomodulin and the D59E variant. Similarly, the dissociation constants for Mg^{2+} at the EF site were identical for both proteins within experimental error.

The minor alterations in affinity for Ca^{2+} and Mg^{2+} at the CD site wrought by the D59E mutation might seem paradoxical in view of the marked sensitivity of the Eu^{3+} luminescence properties to the same substitution. It should be noted, however, that the two experimental techniques are not reporting on identical thermodynamic quantities. The Eu^{3+} $^7F_0 \rightarrow {}^5D_0$ transition monitors interactions between the bound ion and the coordinating ligands and, thus, is primarily a barometer of the enthalpic contribution to the free energy of the ion-protein complex. Since the substitution of glutamate for aspartate at position 59 replaces indirect coordination via a bridging water molecule by direct coordination through a carboxylate, the mutation is expected to have a significant effect on the $^7F_0 \rightarrow {}^5D_0$ spectral properties. The relative affinity of the CD domain for Ca^{2+} and Mg^{2+}, on the other hand, will be influenced by entropic considerations as well, such as how completely solvent is excluded from the site when each ion is bound. Noncoordinating residues are likely to be important determinants of solvent exclusion, since the size of the binding pocket and the coordination geometry will be dictated by tertiary structural interactions involving the binding loop, adjacent helical segments, and the rest of the polypeptide chain. Thus, the results afforded by the two lines of inquiry are not incompatible and, in fact, illustrate why both types of measurement are necessary for a complete analysis of the ion-binding properties.

MacManus *et al.* (64) have also examined the consequences of the D59E mutation, employing UV absorbance, fluorescence, and NMR measurements. These investigators find that, in contrast to the wild-type protein, the spectral properties of the site-specific variant are sensitive to the binding of Mg^{2+} at the CD domain. In light of our binding measurements, their result suggests that the D59E substitution facilitates Mg^{2+}-provoked conformational changes in the protein but does not profoundly alter the observed affinity of the CD site for the ion.

The changes in the Ca^{2+} and Mg^{2+} dissociation constants resulting from the D59E mutation are small, and their significance might have gone unrecognized had we not already seen the Eu^{3+} data. The relative ease of performing the lanthanide luminescence experiments, in comparison with conventional Ca^{2+} binding measurements, and their sensitivity to subtle changes in ligation make the technique well suited for screening our bank of site-specific variants for significant alterations in metal ion-binding characteristics.

Despite the aforementioned changes, the Eu^{3+} luminescence properties of D59E still differ substantially from those of rat parvalbumin. Moreover, the dissociation constants for Ca^{2+} and Mg^{2+} in D59E are little changed from wild-type oncomodulin. These observations are significant since the coordinating residues are identical in D59E and rat parvalbumin. The clear-cut implication is that residues besides those directly involved in ion binding are important in determining the binding characteristics of a given calcium-binding domain. We are currently investigating the significance of other sequence nonidentities in the CD binding loop and in the adjacent helical segments.

Acknowledgments—We gratefully acknowledge the support of the College of Arts and Sciences Research Center, the Biomedical Research Support Committee, and the Department of Chemistry. We thank Dr. John P. MacManus for generously providing us with the nucleotide sequence of oncomodulin prior to publication. We also wish to thank Molycorp, Inc., for supplying one of us (E. R. B.) with a sample of Eu_2O_3. Finally, we acknowledge the technical assistance of Daniel Taylor and Thomas Hurdis.

REFERENCES

1. Kretsinger, R. H. (1980) *CRC Crit. Rev. Biochem.* **8**, 119–174
2. Seamon, K. B., and Kretsinger, R. H. (1983) in *Calcium in Biology* (Spiro, T. G., ed) pp. 3–45, John Wiley and Sons, New York
3. Kretsinger, R. H. (1979) in *Calcium-binding Proteins and Calcium Function* (Wasserman, R. H., Corradino, R., Carafoli, E., Kretsinger, R. H., MacLennan, D., and Siegel, F., eds) pp. 63–72, Elsevier Scientific Publishing Co., New York

4. Szbenyi, D. M. E., Obendorf, S. K., and Moffat, K. (1981) *Nature* **294,** 327–332
5. Herzberg, O., and James, M. N. G. (1985) *Nature* **313,** 653–659
6. Sundaralingam, M., Bergstrom, R., Strasburg, G., Rao, S. T., Roychowdhury, P., Greaser, M., and Wang, B. C. (1985) *Science* **227,** 945–948
7. Babu, Y. S., Sack, J. S., Greenhough, T. G., Bugg, C. E., Means, A. R., and Cook, W. J. (1985) *Nature* **315,** 37–40
8. Haiech, J., Derancourt, J., Pechère, J.-F., and Demaille, J. G. (1979) *Biochemistry* **18,** 2752–2758
9. Haiech, J., Klee, C. B., and Demaille, J. G. (1981) *Biochemistry* **20,** 3890–3897
10. MacManus, J. P., and Whitfield, J. F. (1983) *Calcium Cell Function* **4,** 411–440
11. MacManus, J. P., Whitfield, J. F., Boynton, A. L., Durkin, J. P., and Swierenga, S. H. H. (1982) *Oncodev. Biol. Med.* **3,** 79–90
12. Durkin, J. P., Brewer, L. M., and MacManus, J. P. (1983) *Cancer Res.* **43,** 5390–5394
13. MacManus, J. P. (1981) *FEBS Lett.* **126,** 245–249
14. Mutus, B., Karrupiah, N., Sharma, R. K., and MacManus, J. P. (1985) *Biochem. Biophys. Res. Commun.* **131,** 500–506
15. Brewer, L. M., Durkin, J. P., and MacManus, J. P. (1984) *J. Histochem. Cytochem.* **32,** 1009–1016
16. Brewer, L. M. and MacManus, J. P. (1985) *Dev. Biol.* **112,** 49–58
17. MacManus, J. P., Brewer, L. M., and Whitfield, J. F. (1985) *Cancer Lett.* **27,** 145–151
18. MacManus, J. P., Szabo, A. G., and Williams, R. E. (1984) *Biochem. J.* **220,** 261–268
19. Mutus, B., Flohr, E. J., and MacManus, J. P. (1985) *Can. J. Biochem. Cell Biol.* **63,** 998–1002
20. Williams, T. C., Corson, D. C., Sykes, B. D., and MacManus, J. P. (1987) *J. Biol. Chem.* **262,** 6248–6256
21. Herzberg, O., and James, M. N. G. (1985) *Biochemistry* **24,** 5298–5302
22. Berchtold, M. W., Heizmann, C. W., and Wilson, K. J. (1982) *Eur. J. Biochem.* **127,** 381–389
23. Epstein, P., Means, A. R., and Berchtold, M. W. (1986) *J. Biol. Chem.* **261,** 5886–5891
24. Gillen, M. F., Banville, D., Rutledge, R. G., Narang, S., Seligy, V. L., Whitfield, J. F., and MacManus, J. P. (1987) *J. Biol. Chem.* **262,** 5308–5312
25. Corson, D. C., Williams, T. C., and Sykes, B. D. (1983) *Biochemistry* **22,** 5882–5889
26. Williams, T. C., Corson, D. C., and Sykes, B. D. (1984) *J. Am. Chem. Soc.* **106,** 5698–5702
27. Henzl, M. T., and Birnbaum, E. R. (1988) *J. Biol. Chem.* **263,** 10674–10680
28. Lyle, S. J., and Rahman, M. (1963) *Talanta* **10,** 1177–1182
29. Laemmli, U. K. (1970) *Nature* **227,** 680–685
30. Morrissey, J. H. (1981) *Anal. Biochem.* **117,** 302–310
31. Creighton, T. E. (1986) *Methods Enzymol.* **131,** 156–172
32. Maniatis, T., Fritsch, E. F., and Sambrook, J. (1982) *Molecular Cloning: A Laboratory Manual,* Cold Spring Harbor Laboratory, Cold Spring Harbor, NY
33. Hurn, B. A. L., and Chantler, S. M. (1980) *Methods Enzymol.* **70,** 104–142
34. Erickson, P., Minier, L., and Lasher, R. (1982) *J. Immunol. Methods* **51,** 241–249
35. Batteiger, B., Newhall, W. J., and Jones, R. B. (1982) *J. Immunol. Methods* **55,** 297–307
36. Helfman, D. M., Feramisco, J. R., Fiddes, J. C., Thomas, G. P., and Hughes, S. H. (1983) *Proc. Natl. Acad. Sci. U. S. A.* **80,** 31–35
37. Henzl, M. T., McCubbin, W. D., Kay, C. M., and Birnbaum, E. R. (1985) *J. Biol. Chem.* **260,** 8447–8455
38. Colowick, S. P., and Womack, F. C. (1968) *J. Biol. Chem.* **244,** 774–777
39. Haner, M., Henzl, M. T., Raissouni, B., and Birnbaum, E. R. (1984) *Anal. Biochem.* **138,** 229–234
40. Gubler, U., and Hoffman, B. J. (1983) *Gene (Amst.)* **25,** 263–269
41. MacManus, J. P. (1980) *Biochim. Biophys. Acta* **621,** 296–304
42. Kunkel, T. A. (1985) *Proc. Natl. Acad. Sci. U. S. A.* **82,** 488–492
43. Kunkel, T. A., Roberts, J. D., and Zakour, R. A. (1987) *Methods Enzymol.* **154,** 367–382
44. Norris, K., Norris, F., Christiansen, L., and Fiil, N. (1983) *Nucleic Acids Res.* **11,** 5103–5113
45. Holmes, D. S., and Quigley, M. (1981) *Anal. Biochem.* **114,** 193–197
46. Samelson, H., Brecher, C., and Lempicki, A. (1966) *J. Mol. Spectrosc.* **19,** 349–371
47. Horrocks, W. DeW., Jr., and Sudnick, D. R. (1979) *Science* **206,** 1194–1196
48. Wang, C.-L. A., Leavis, P. C., Horrocks, W. DeW., Jr., and Gergely, J. (1981) *Biochemistry* **20,** 2439–2444
49. Wang, C.-L. A., Aquaron, R. R., Leavis, P. C., and Gergely, J. (1982) *Eur. J. Biochem.* **124,** 7–12
50. Mulqueen, P., Tingey, J. M., and Horrocks, W. DeW., Jr. (1985) *Biochemistry* **24,** 6639–6645
51. van Scharrenburg, G. J. M., Slotboom, A. J., De Haas, G. H., Mulqueen, P., Breen, P. J., and Horrocks, W. DeW., Jr. (1985) *Biochemistry* **24,** 334–339
52. Horrocks, W. DeW., Jr., and Collier, W. E. (1981) *J. Am. Chem. Soc.* **103,** 2856–2862
53. Rhee, J.-J., Sudnick, D. R., Arkle, V. K., and Horrocks, W. DeW., Jr. (1981) *Biochemistry* **20,** 3328–3334
54. Breen, P. J., Hild, E. K., and Horrocks, W. DeW., Jr. (1985) *Biochemistry* **24,** 4991–4997
55. Henzl, M. T., Hapak, R. C., and Birnbaum, E. R. (1986) *Biochim. Biophys. Acta* **872,** 16–23
56. Potter, J. D., Johnson, J. D., Dedman, J. R., Schreiber, W. E., Mandel, F., Jackson, R. L., and Means, S. R. (1977) in *Calcium-binding Proteins and Calcium Function* (Wasserman, R. H., Corradino, R. A., Carafoli, E., Kretsinger, R. H., MacLennan, D. H., and Siegel, F. L., eds) pp. 239–249, Elsevier Scientific Publishing Co., New York
57. Moeschler, H. J., Schaer, J.-J., and Cox, J. A. (1980) *Eur. J. Biochem.* **111,** 73–78
58. Reid, R. E., Gariépy, J., Saund, A. K., and Hodges, R. S. (1981) *J. Biol. Chem.* **256,** 2742–2751
59. Derancourt, J., Haiech, J., and Pechère, J. F. (1978) *Biochim. Biophys. Acta* **532,** 373–375
60. Martin, R. B. (1983) in *Calcium in Biology* (Spiro, T. G., ed) pp. 237–270, John Wiley and Sons, New York
61. Albin, M., and Horrocks, W. DeW., Jr. (1985) *Inorg. Chem.* **24,** 895–900
62. Rinaldi, M. L., Haiech, J., Pavlovitch, J., Rizk, M., Ferraz, C., Derancourt, J., and Demaille, J. G. (1982) *Biochemistry* **21,** 4805–4810
63. Goodman, M., Pechere, J.-F., Haiech, J., and Demaille, J. G. (1979) *J. Mol. Evol.* **13,** 331–352
64. MacManus, J. P., Hutnik, C. M. L., Sykes, B. D., Szabo, A. F., Williams, T. C., and Banville, D. (1989) *J. Biol. Chem.* **264,** 3470–3477